Published in final edited form as:

Cell Microbiol. 2020 September ; 22(9): e13217. doi:10.1111/cmi.13217.

Media Matters! Alterations in the loading and release of *Histoplasma capsulatum* extracellular vesicles in response to different nutritional milieus.

Levi G. Cleare[1], **Daniel Zamith**[1], **Heino M. Heyman**[2,#], **Sneha P. Couvillion**[2], **Leonardo Nimrichter**[3], **Marcio L. Rodrigues**[3,4], **Ernesto S. Nakayasu**[2], **Joshua D. Nosanchuk**[1,*]

[1]Department of Medicine (Division of Infectious Diseases) and Department of Microbiology and Immunology, Albert Einstein College of Medicine, Bronx, NY 10461 USA

[2]Biological Sciences Division, Pacific Northwest National Laboratory, Richland, WA 99352, USA

[3]Instituto de Microbiologia Paulo de Góes, Universidade Federal do Rio de Janeiro (UFRJ), Rio de Janeiro, RJ, Brazil

[4]Instituto Carlos Chagas, Fundação Oswaldo Cruz (Fiocruz), Curitiba, Brazil

Abstract

Histoplasma capsulatum is a dimorphic fungus that most frequently causes pneumonia, but can also disseminate and proliferate in diverse tissues. *H. capsulatum* has a complex secretion system that mediates the release of macromolecule-degrading enzymes and virulence factors. The formation and release of extracellular vesicles (EVs) are an important mechanism for non-conventional secretion in both ascomycetes and basidiomycetes. *H. capsulatum* EVs contain diverse proteins associated with virulence and are immunologically active. Despite the growing knowledge of EVs from *H. capsulatum* and other pathogenic fungi, the extent that changes in the environment impact the sorting of organic molecules in EVs has not been investigated. In this study, we cultivated *H. capsulatum* with distinct culture media to investigate the potential plasticity in EV loading in response to differences in nutrition. Our findings reveal that nutrition plays an important role in EV loading and formation, which may translate into differences in biological activities of these fungi in various fluids and tissues.

Keywords

Histoplasma capsulatum; histoplasmosis; dimorphic fungus; culture media; proteomics; lipidomics; metabolomics; BHI; Ham's F12; RPMI; extracellular vesicles; USA

*Correspondence author: josh.nosanchuk@einstein.yu.edu.

#Current address: Heino M. Heyman, Bruker Daltonics, Inc., Billerica, Massachusetts, USA

J.D.N. conceived the presented idea. L.C. carried out the experiments to isolate extracellular vesicles. L.C. and D.Z. characterized the vesicles. H.M., S.C., and E.N. performed omic analysis. L.N., M.R., and E.N. contributed to the interpretation of results. L.C. and D.Z. wrote the manuscript with input from all authors.

Conflict of Interest

We declare that there are no conflicts of interest.

Introduction

Extracellular vesicles (EVs) have been identified in all biological kingdoms. Fungal EVs were first described in *Cryptococcus neoformans*, in 2007, as a trans-cell wall transport mechanism that effectively delivers macromolecules to the extracellular environment (1). The following year, this process was extended to several additional fungi, which demonstrates that this remarkable process is ancient, given that both Basidiomycota and Ascomycota generated EVs (2). Furthermore, research on fungal EVs reveals that their contents contain diverse components associated with fungal virulence, and are recognized by individuals previously infected with the specific fungus (1, 2). Since then, EVs have been shown to modify host effector responses, including altering macrophage activation, macrophage polarization and host susceptibility to fungal challenge (3). Histoplasmosis, caused by the dimorphic fungus *Histoplasma capsulatum*, is a significant cause of mortality and morbidity on the global stage, and it is the most common cause of fungal pneumonia in the U.S.A (4, 5). Thermally dimorphic fungi are remarkable among fungal pathogens because they cause disease in humans with normal or impaired immune defenses (6). *H. capsulatum* persists in soil as well as bird and bat excretes (7). Disruption of soil by natural events or by human activities, such as construction, leads to aerosolization of conidia and hyphal fragments. When inhaled into the lungs of a mammalian host (37°C), these infectious propagules convert into pathogenic yeast to cause pneumonia. Once infection is established in the lungs, the yeast can widely disseminate and produce EVs into the host environment (8). We have previously demonstrated that *H. capsulatum* produces EVs containing a vast array of proteins, lipids and carbohydrates (2). Remarkably, the packaging and release of *H. capsulatum* EVs can be dynamically regulated by the binding of antibody to the cell surface of this yeast (8, 9) which suggests that other stressors may dramatically impact EV biogenesis and, consequently, composition.

H. capsulatum is commonly cultivated in several different rich or nutritionally restrictive media. However, during infection, the fungus can reside and flourish in fluid and tissue environments throughout the body, ranging from the blood and cerebral spinal fluid to the lung and brain, and variables such as the pH, oxygen content and available nutrients are different in these diverse locations. In this study, we examined the impact of three standard growth media on EVs content loading, which we hypothesized would alter EVs characteristics and payloads. Given that there are significantly different nutritional conditions that *H. capsulatum* encounters during disseminated disease, exploring variations in EV production in different nutritional environments may lead to insights into EV plasticity and pathogenesis.

Experimental Procedures

Fungal culture

The *H. capsulatum* wild-type strain G217B (ATCC 26032) was used for all experiments. The strain has been maintained at −80°C and cultivated in liquid medium at 37°C prior to use. The media used for *H. capsulatum* cultivation were: brain heart infusion (BHI; BD Diagnostic System), Ham's F-12 Nutrient Mixture (Thermofisher) supplemented with glucose (1.82g/L), glutamic acid (1 g/L), HEPES (6.5 g/L) and L-Cysteine (8.4 mg/L)

referenced from a defined medium called Histoplasma macrophage medium (10), and Roswell Park Memorial Institute 1640 (RPMI; Corning Cellgro) supplemented with 1% Nutridoma (Roche Applied Science). BHI and Ham's F12 are generally considered rich nutritional growth media whereas RPMI is a standard medium used for cell culture.

EV isolation

H. capsulatum G217B was inoculated into Ham's F-12 medium and incubated at 37°C with rotary agitation at 150 rpm. Fifty mL of yeast cell culture in each media were adjusted to 0.05 Optical Density (OD) and further cultivated for 4 days at 37°C with rotary agitation. Culture supernatants were collected by centrifugation for 10 minutes at 4,000 x *g* for 20 minutes at 4°C. The supernatants were then filtered through a 0.45 micrometer filter, then concentrated (~15 times) in an Amicon filtration system with a 100-kDa cutoff membrane (Millipore). The collected concentrates were then subjected to 150.000 × *g*ultracentrifugation (Beckman Coulter Optima TLX) with a TLA 100.3 rotor at 4°C, (Beckman Coulter) 2 times for 1 h each, with a suspension step after the first hour. EV pellets were suspended in 200 μL of sterile PBS.

EV Analysis

After isolation, EVs were quantified for protein and ergosterol by indirect methods. Protein quantification was determined by BCA Protein Assay Reagent kit (Pierce) and sterol quantification determined by Amplex Red Sterol assay kit (Invitrogen). EVs were analyzed by Dynamic Light Scattering (DLS) for vesicle size (2).

Multi-omics analysis

EVs were submitted to Metabolite, Protein and Lipid Extraction (MPLEx) and analyzed well-established a protocol as previously tested for different samples, including EVs and fungal cells (11–14). Briefly, EVs were resuspended in 25 μL of 50 mM NH_4HCO_3 and extracted with 5 volumes of chloroforrmmethanol solution (2:1, v:v). Samples were vortexed, incubated on ice for 5 min and centrifuged for 5 min at 12,000 xg at 4°C to separate the extracts into different solvent layers. Metabolites, proteins and lipids were collected into separate vials and submitted to specific mass spectrometry analysis pipelines. The hydrophilic metabolite layer was dried in a vacuum centrifuge prior to be derivatized with methoxyamine and N-methyl-N-(trimethylsilyl)trifluoroacetamide, and analyzed in a GC 7890A coupled with a single quadrupole MSD 5975C (Agilent Technologies, Inc) (15). Data files were processed with Metabolite Detector (16) for extracting peaks and deconvoluting the fragmentation spectra. Identifications were done by matching against the Fiehn Metabolomics Retention Time Locked (RTL) Library (17). Lipids were dried in a vacuum centrifuged and dissolved in pure methanol before being analyzed by liquid chromatography-tandem mass spectrometry (LC-MS/MS) on an Orbitrap mass spectrometer (Thermo Fisher Scientific) and identifications were done with the LIQUID software (18). Peak areas of manually validated lipid species were extracted with MZmine 2.0 (19). The protein layer is reduced with dithiothreitol, alkylated with iodoacetamide and digested with trypsin (9). Digested peptides were analyzed LC-MS/MS on a Q-Exactive mass spectrometer (Thermo Fisher Scientific). Collected data was processed with MaxQuant (v1.5.5.1) (20) by searching against the *H. capsulatum* G186AR sequences downloaded

from the Uniprot Knowledge Base on August 15, 2016. Methionine oxidation and protein N-terminal acetylation were considered as variable modifications, while cysteine carbamidomethylation was set as fixed modifications. The label-free quantification (LFQ) values were used for quantitative analysis.

Statistical Analysis

Statistical analyses were done by using one-way ANOVA, followed by Tukey's comparison test and analysis. Function-enrichment analysis was done by annotating *H. capsulatum* sequences by blasting against the KEGG database (21) testing for enrichment using Fisher's exact test. Lipid ontology analysis was done using Lipid Mini-On (22). Asterisks presented in figures represent P-values, one asterisk for a value < 0.05, and two asterisks for a value < 0.01.

Results

Protein and ergosterol content and size of EV

EVs isolated from *H. capsulatum* cultivated in BHI, Ham's F-12, and RPMI are referred hereafter as EV-BHI, EV-Ham's, and EV-RPMI, respectively. EV-Ham's presented the highest yield of both total protein and ergosterol. EV-BHI and EV-RPMI had comparable amounts of protein and ergosterol, which were less than that observed for EV-Ham's (Fig. 1A and 1B).

Figure 2 presents the size of the EVs isolated from each medium. DLS analysis of fungal EVs reveals 2 population sizes of EVs in the three conditions, which is similar to prior reports for *H. capsulatum* and other fungi (23). The small EVs population range from 40 to 70 nm, and the larger from 200 to 500 nm. There was a difference in population sizes of the small and large EVs between EV-BHI and EV-Ham's, otherwise all EVs are within range of previously described fungal EVs.

Proteomic analysis of EVs

Fungal EVs contain diverse proteins in their cargo, including molecules that act as virulence factors (24). Hence, we analyzed the protein content of EVs released from *H. capsulatum* cultured in distinct media conditions to determine if differences in nutrition altered the presence of potentially biologically active proteins. The proteomic analysis identified approximately 2,000 proteins, and 270 were significantly altered among the distinct growth conditions. Some of these proteins were found to be involved in key pathways, particularly cellular product synthesis and metabolism. Table 1 shows proteins included in important KEGG pathways, classified by fold enrichment, some of which we will refer to later in the text.

The proteins were grouped into four different clusters according to their abundance in BHI [group 4], RPMI [group 3], Ham's [group 2] and BHI and Ham's [group 1]. There were more abundant proteins in EV-Ham's, and a greater variance in EV-BHI within the replicates.

EV-BHI and EV-Ham's presented similar protein yields in group 4, which contains most of the protein yields. However, the majority of altered proteins were significantly abundant in EV-Ham's compared to EV-BHI and EV-RPMI. The most variation in protein alteration between the EV-BHI, EV-Ham's, and EV-RPMI occurred in group 1. Proteins from EV-RPMI were most abundant in group 2 (Figure 2).

The proteins abundant in both EV-Ham's and EV-BHI were in the largest cluster in the heatmap (Fig. 2). In this cluster, important proteins involved with chitin metabolism were found, including chitin synthase (C0NZK3, C0NSP8 and C0NDJ0) and chitinase (C0NSB6). Also, enzymes involved with host response modulation were detected, such as peroxidase (C0NND7) and alkaline phosphatase (C0NBI7). Lipid metabolism enzymes were also abundant in these EVs, such as carnitine (C0NWZ6), long-chain-fatty-acid-CoA ligase (C0P0B7), acetyl-CoA carboxylase (C0NM24). EV-BHI presented an abundance of sugar metabolism-related enzymes, including alpha-glucosidase (C0NEI5) and glucosidase I (C0NHJ7). Interestingly, EV-RPMI didn't present abundance of enzymes involved in cell wall remodeling and the only lipid-related abundant protein in EV-RPMI was the Inositol-3-phosphate synthase (C0NLK4). Among the proteins exported in EV-Ham's, the high affinity copper transporter (C0NSW0), abundant only in EV-Ham's. EV-Ham's had the highest abundance of siderochrome-iron uptake transporter (C0NX70), as well as V-type proton ATPase subunit A (C0NJV7).

Lipidomic analysis of EVs

The lipidomic analysis detected 100 lipids, with significant alterations in 44 lipids among the different media conditions. Among the significantly altered lipids, the greatest variety was found in EV-Ham's, in mostly species of phosphatidylethanolamine (PE) and phosphatidylcholine (PC). Figure 4A shows a heatmap with the significantly altered lipids. The heatmap shows 2 distinct clusters of altered lipids. The biggest cluster shows lipids that were abundant in EV-Ham's, and the smaller cluster shows EV-RPMI abundant lipids. Lipids abundant in EV-BHI are present in both clusters, except for the sphingomyelins, which were abundant only in EV-BHI.

EV-BHI presented the largest variety in class of lipids among the tested conditions, including several species of sphingomyelin, one ceramide, and a phosphoinositol ceramide. Phosphoinositol ceramide was also abundant in both EV-BHI and EV-RPMI. EV-Ham's yielded significantly lower abundances of triacylglycerides (TG) and diacylglycerides (DG) compared to EV-BHI and EV-RPMI (Fig. 4B–4C). Most of the abundant lipids found in EV-RPMI (~78%) had saturated fatty acids (FA), while ~70% of the FA found in lipids abundant in EV-Ham's were unsaturated. Regarding the presence of unsaturated lipids, EV-BHI's lipids were in an intermediary level between the other conditions. (Fig. 3E).

Lysophospholipids were more abundant in EV-RPMI, especially lysophosphatidylcholine (LysoPC). LysoPCs were more abundant in EV-RPMI and EV-Ham's compared to EV-BHI (Figure 5). One species of lysophosphatidylethanolamine (LysoPE) was present in EV-RPMI and EV-Ham's. The few odd-chain FA found to be abundant in our analysis were present mostly in EV-Ham's, and none of them were lysophospholipids.

Metabolomic analysis of EVs

Carbohydrate metabolites vary in the EVs from each condition. EV-Ham's presents the most abundant D-glucose content (Figure 6); however, the amount of D-glucose present in the media BHI and RPMI was not translated in the abundance of this carbohydrate in EV generated in their presence. Carbohydrates such as maltose, isomaltose, D-allose, and pyruvic acid, also associated with energy storage and production, were most abundantly found in EV-Hams. Although EV-Ham's presents a majority of the carbohydrate metabolites, EV-BHI presents more abundance of trehalose and fructose. EV-BHI presents the most abundance of trehalose, and the least abundance of glucose and pyruvic acid compared to EV-Hams and EV-RPMI. EV-BHI had the highest abundance of L-ornithine even though the abundance of arginase was the same among all tested conditions. The high abundance of ethanolamine in EV-Ham's reflects the lipidomic profile of these EV, where phospholipids containing ethanolamine represent more than half of the lipid classes found in this experimental condition.

Discussion

Compositional analyses of fungal EVs are essential to the understanding of how these extracellular compartments exert their functions. For instance, there is now concrete evidence that fungal EVs modulate virulence transfer between distinct fungal strains (25) activation of immune cells (26–29), prion transfer(30), and drug resistance in biofilms(31) among other functions. However, in the absolute majority of the studies showing fundamental biological functions of EVs, the bioactive vesicular components remained unknown. Therefore, knowledge on the compositional diversity of fungal EVs directly impact the understanding of their functions in nature, but also the design of EV-based biotechnological tools, including vaccines and therapeutic agents.

The initial description of EVs in *C. neoformans* has been followed by numerous interesting reports of EVs produced in other important human pathogenic fungi. Although EVs can also be released from non-pathogenic fungi, as well as in organisms from other kingdoms, their release by pathogenic fungi has called the attention of microbiologists mainly because these EVs can carry virulence factors (24). Although many aspects about fungal EV biology and their effects on hosts have been addressed to date, it is still poorly understood whether environmental conditions modulate EV cargo. Previously we partially explored this question, comparing EVs from *H. capsulatum* released in the presence or absence of monoclonal antibodies against a heat-shock protein exposed on the surface of *H. capsulatum* and found that antibody dynamically altered EV cargo in a dose-dependent manner (32). In the current work we analyzed the content of EV released from *H. capsulatum* cultivated in distinct media conditions, to evaluate EV plasticity regarding their cargo and constitution in response to nutrition.

Each of the medium tested in our study has a different chemical composition. BHI is a nutritious, buffered culture medium that contains infusions of brain and heart tissue and peptones to supply protein and other nutrients necessary to support the growth of fastidious and nonfastidious microorganisms (33). Ham's F-12 was designed for serum-free single-cell plating of Chinese Hamster Ovary (CHO) cells, and has been used for a wide range of

mammalian cells as well as bacteria and fungi. Ham's F-12 Nutrient Mixture medium supplements were referenced from a defined medium called *Histoplasma* macrophage medium aforementioned. RPMI is unique from other medium because it contains the reducing agent glutathione and high concentrations of vitamins, inositol and choline. A full description of media components has been included in supplemental Table S1. Nutridoma, was added to RPMI as a supplement. It consists as a biochemically defined replacement for Fetal Bovine Serum (FBS). We observed the growth of *H. capsulatum* based on OD and were able to determine when the fungus reached stationary phase growth. This stage of growth was determined to be 96 hours after initial inoculation in each of the three media.

Proteins and lipids, among other organic molecules, are present in *H. capsulatum* EVs, some of which are closely linked to virulence during infection and disease. EV-Ham's had the highest amount of both protein and ergosterol. However, these EVs were the smallest in size among the tested conditions, being smaller than EV-BHI and statistically similar to EV-RPMI, suggesting that EV-Ham's are either produced in higher amounts than the other conditions, or that they are "denser" than EVs from the other media. Application of methods that could directly measure EV counts in each medium could answer this question in the future. Following the total protein content, the proteomic analysis showed that most of the altered proteins were abundantly found in EV-Ham's, as EV-RPMI had only a few proteins significantly more abundant than the other conditions. Interestingly, EV-RPMI had lower abundance of proteins associated with carbohydrate and polysaccharide metabolism in Cluster 4 (Figure 3) even though RPMI medium contains higher levels of glucose (10%) compared to Ham's F-12. EV-BHI showed some inconsistencies between its replicates, probably because of the nature of the medium, where different animals' brain and heart material are present, so variations between distinct lots might occur. It may be possible that a few of the proteins analyzed were directly from the media itself. However, when we subjected the different media without fungal inoculation to our EV isolation protocol and tested residual fluid by DLS, there were no EVs detected (data not shown). In comparison, Ham's F-12 medium was the most consistent condition where the yeast cells exported, through EVs, the largest variety of proteins. This feature might reflect how suitable this medium is on the growth of *H. capsulatum* for experiments that involve host-pathogen interactions. Copper and some other micronutrients in the host environment can become toxic to host pathogens. Among the proteins exported in EV-Ham's, the high affinity copper transporter (C0NSW0), abundant only in EV-Ham's, is an important immune subversion protein mechanism as one of the strategies used by host phagocytes to inhibit the viability of intracellular *H. capsulatum* is to reduce the access of copper into the phagosome (34). Therefore, the presence of this metal transporter can protect the host pathogen by inhibiting the use of copper in host defense cells. The presence of this metal transporter can be due to the fact that Ham's F-12 medium contains the micronutrient metal cupric sulfate, while the other media do not. EV-Ham's had the highest abundance of siderochrome-iron uptake transporter (C0NX70), a protein essential for the fungus to survive in environments with low iron availability. Iron acquisition in *H. capsulatum* also relies on the cooperative action of proton ATPases as the V-type proton ATPase subunit A (C0NJV7), which is also consistently abundant in EV-Ham's.

The lipid profile of EV cultivated in distinct media was remarkably distinct. EV-BHI incorporated or synthesized different classes of lipids, as ceramides and sphingomyelins were present almost in an exclusive way in this condition. Ham's F12 and RPMI are more defined media, while BHI has brain and heart material different animals, and it is the only one of these media that actually carries lipids, with the exception of linoleic acid present in Ham's. Sphingomyelins are not synthesized by yeast cells due to the lack of sphingomyelin synthase in fungi (35), but they are probably up taken from media and were loaded into EVs. Nevertheless, polyunsaturated FA were consistently found only in EV-Ham's, as well as the highest abundance of diunsaturated FA. The condition with fewer unsaturated FA was also found in EV-Ham's. Almost 80% of the abundant FA in EV-RPMI were unsaturated, and accordingly the ergosterol presence in these EV was quite low. EV-Hams having fewer unsaturated FA is presumably balanced by the highest amount of ergosterol, limiting the EVs membrane fluidity. EV-RPMI also presented the highest abundance of lysophospholipids, despite the equal abundance of phospholipases in all the conditions. This data suggests that in this condition, the lysis of phospholipids would take place before the assembling of EV by intracellular phospholipases, or even in the extracellular milieu by secreted phospholipases non associated with EVs. In any case, differences in lipid composition induced by growth conditions might impact virulence and/or immunological potential. For instance, fungal EVs enriched with the immunogenic glycolipid ergosterylglucoside induced protection of the invertebrate host *Galleria mellonella* against a lethal challenge with *C. neoformans* (26).

Carbohydrate metabolites found within the EVs were also interesting. The glucose in each medium is described as follows: BHI medium provides 3 g/L of dextrose, Ham's medium is supplemented with 1.82 g/L of glucose, and RPMI 1640 has 2 g/L of glucose. EV-Ham's presented the highest amount of carbohydrates associated with energy production and storage. This could possibly be due to the high amounts received from the medium. Besides energy production, EV-RPMI also presented high amounts of carbohydrates associated with energy production. Trehalose, a stress tolerance related carbohydrate (36, 37), had increased abundance in EV-BHI. It has also been reported to be involved in mechanisms like substituting water molecules in cell membrane to protect from desiccation and freezing damage, conferring thermotolerance by stabilizing proteins during heat shock, and acting as a compatible osmolyte (38). Other functions of trehalose include being an alternative carbon source for filamentous fungi, especially in glycogen deficient environments (39). The high abundance of trehalose in EV-BHI can be related to the medium composition of mammalian ingredients, compounded with host temperate growth conditions. The presence of L-ornithine in EV-BHI does not reflect the abundance of arginase in these EVs, as this enzyme was equally abundant among all conditions. This pattern suggests that although it is possible to have L-ornithine synthesis inside EVs, the differential abundance found in EV-BHI was probably due to an increased synthesis of this metabolite inside the yeast cells or even a differential sorting during EV biogenesis.

Fungal EV cargo can be modulated by host factors, such as specific antibody binding to fungal cell surface proteins (9). However, the impact of media condition on EV biogenesis has not been examined. With this study, we demonstrate remarkable alterations of fungal EV cargo loading and EV release based on the available nutrients for fungal growth, and begin

to reveal how these conditions can be related to cell-host interactions. These findings provide a strong proof of concept that that different host and environmental conditions, in this case media, can induce changes in the EV composition that may potentially lead to a more or less virulent state of a fungus.

Supplementary Material

Refer to Web version on PubMed Central for supplementary material.

Acknowledgements

J.D.N. was supported in part by NIH R01AI052733 and R21AI124797. E.S.N. was partially supported by NIH R21AI124797. Parts of this work were performed in the Environmental Molecular Science Laboratory, a U.S. Department of Energy (DOE) national scientific user facility at Pacific Northwest National Laboratory (PNNL) in Richland, WA. MLR and LN are supported by grants from the Brazilian agency Conselho Nacional de Desenvolvimento Cientifico e Tecnologico (CNPq, grants 405520/2018-2, 440015/2018-9, and 301304/2017-3 to M.L.R.; 311179/2017-7 and 408711/2017-7 to L.N.) and Fiocruz (grants VPPCB-007-FIO-18-2-57 and VPPIS-001-FIO-18-66 to M.L.R,). We also acknowledge support from the Instituto Nacional de Ciência e Tecnologia de Inovação em Doenças de Populações Negligenciadas (INCT-IDPN). M.L.R. is currently on leave from the position of Associate Professor at the Microbiology Institute of the Federal University of Rio de Janeiro, Brazil.

References

1. Rodrigues ML, Nimrichter L, Oliveira DL, Frases S, Miranda K, Zaragoza O, et al. Vesicular polysaccharide export in *Cryptococcus neoformans* is a eukaryotic solution to the problem of fungal trans-cell wall transport. Eukaryot Cell. 2007;6(1):48–59. [PubMed: 17114598]
2. Albuquerque PC, Nakayasu ES, Rodrigues ML, Frases S, Casadevall A, Zancope-Oliveira RM, et al. Vesicular transport in *Histoplasma capsulatum*: an effective mechanism for trans-cell wall transfer of proteins and lipids in ascomycetes. Cellular microbiology. 2008;10(8):1695–710. [PubMed: 18419773]
3. Zamith-Miranda D, Nimrichter L, Rodrigues ML, Nosanchuk JD. Fungal extracellular vesicles: modulating host-pathogen interactions by both the fungus and the host. Microbes Infect. 2018;20(9–10):501–4. [PubMed: 29471026]
4. Cleare LG, Zamith-Miranda D, Nosanchuk JD. Heat Shock Proteins in Histoplasma and Paracoccidioides. Clinical and vaccine immunology : CVI. 2017;24(11).
5. Chu JH, Feudtner C, Heydon K, Walsh TJ, Zaoutis TE. Hospitalizations for endemic mycoses: a population-based national study. Clin Infect Dis. 2006;42(6):822–5. [PubMed: 16477560]
6. Gauthier GM. Fungal Dimorphism and Virulence: Molecular Mechanisms for Temperature Adaptation, Immune Evasion, and In Vivo Survival. Mediators of inflammation. 2017;2017:8.
7. Prevention CfDCa. Fungal Disease 2014 [updated September 30, 2014 Available from: https://www.cdc.gov/fungal/global/index.html.
8. Baltazar LM, Zamith-Miranda D, Burnet MC, Choi H, Nimrichter L, Nakayasu ES, et al. Concentration-dependent protein loading of extracellular vesicles released by *Histoplasma capsulatum* after antibody treatment and its modulatory action upon macrophages. Scientific reports. 2018;8(1):8065. [PubMed: 29795301]
9. Matos Baltazar L, Nakayasu ES, Sobreira TJ, Choi H, Casadevall A, Nimrichter L, et al. Antibody Binding Alters the Characteristics and Contents of Extracellular Vesicles Released by *Histoplasma capsulatum*. mSphere. 2016;1(2).
10. Worsham PL, Goldman WE. Quantitative plating of *Histoplasma capsulatum* without addition of conditioned medium or siderophores. Journal of medical and veterinary mycology : bi-monthly publication of the International Society for Human and Animal Mycology. 1988;26(3):137–43.

11. Nakayasu ES, Nicora CD, Sims AC, Burnum-Johnson KE, Kim YM, Kyle JE, et al. MPLEx: a Robust and Universal Protocol for Single-Sample Integrative Proteomic, Metabolomic, and Lipidomic Analyses. mSystems. 2016; 1(3).
12. Coelho C, Brown L, Maryam M, Vij R, Smith DFQ, Burnet MC, et al. Listeria monocytogenes virulence factors, including listeriolysin O, are secreted in biologically active extracellular vesicles. The Journal of biological chemistry. 2019;294(4):1202–17. [PubMed: 30504226]
13. Zamith-Miranda D, Heyman HM, Cleare LG, Couvillion SP, Clair GC, Bredeweg EL, et al. Multi-omics Signature of Candida auris, an Emerging and Multidrug-Resistant Pathogen. mSystems. 2019;4(4).
14. Nicora CD, Sims AC, Bloodsworth KJ, Kim YM, Moore RJ, Kyle JE, et al. Metabolite, Protein, and Lipid Extraction (MPLEx): A Method that Simultaneously Inactivates Middle East Respiratory Syndrome Coronavirus and Allows Analysis of Multiple Host Cell Components Following Infection. Methods Mol Biol. 2020;2099:173–94. [PubMed: 31883096]
15. Ansong C, Schrimpe-Rutledge AC, Mitchell HD, Chauhan S, Jones MB, Kim YM, et al. A multi-omic systems approach to elucidating Yersinia virulence mechanisms. Mol Biosyst. 2013;9(1):44–54. [PubMed: 23147219]
16. Hiller K, Hangebrauk J, Jager C, Spura J, Schreiber K, Schomburg D. MetaboliteDetector: comprehensive analysis tool for targeted and nontargeted GC/MS based metabolome analysis. Anal Chem. 2009;81(9):3429–39. [PubMed: 19358599]
17. Kind T, Wohlgemuth G, Lee DY, Lu Y, Palazoglu M, Shahbaz S, et al. FiehnLib: mass spectral and retention index libraries for metabolomics based on quadrupole and time-of-flight gas chromatography/mass spectrometry. Anal Chem. 2009;81(24):10038–48. [PubMed: 19928838]
18. Kyle JE, Crowell KL, Casey CP, Fujimoto GM, Kim S, Dautel SE, et al. LIQUID: an-open source software for identifying lipids in LC-MS/MS-based lipidomics data. Bioinformatics. 2017.
19. Pluskal T, Castillo S, Villar-Briones A, Oresic M. MZmine 2: modular framework for processing, visualizing, and analyzing mass spectrometry-based molecular profile data. BMC Bioinformatics. 2010;11:395. [PubMed: 20650010]
20. Tyanova S, Temu T, Cox J. The MaxQuant computational platform for mass spectrometry-based shotgun proteomics. Nat Protoc. 2016;11(12):2301–19. [PubMed: 27809316]
21. Kanehisa M, Sato Y, Morishima K. BlastKOALA and GhostKOALA: KEGG Tools for Functional Characterization of Genome and Metagenome Sequences. J Mol Biol. 2016;428(4):726–31. [PubMed: 26585406]
22. Clair G, Reehl S, Stratton KG, Monroe ME, Tfaily MM, Ansong C, et al. Lipid Mini-On: Mining and ontology tool for enrichment analysis of lipidomic data. Bioinformatics. 2019.
23. Joffe LS, Nimrichter L, Rodrigues ML, Del Poeta M. Potential Roles of Fungal Extracellular Vesicles during Infection. mSphere. 2016;1(4).
24. Rodrigues ML, Godinho RM, Zamith-Miranda D, Nimrichter L. Traveling into Outer Space: Unanswered Questions about Fungal Extracellular Vesicles. PLoS pathogens. 2015;11(12):e1005240. [PubMed: 26633018]
25. Bielska E, Sisquella MA, Aldeieg M, Birch C, O'Donoghue EJ, May RC. Pathogen-derived extracellular vesicles mediate virulence in the fatal human pathogen Cryptococcus gattii. Nature communications. 2018;9(1):1556.
26. Colombo AC, Rella A, Normile T, Joffe LS, Tavares PM, de SAGR, et al. *Cryptococcus neoformans* Glucuronoxylomannan and Sterylglucoside Are Required for Host Protection in an Animal Vaccination Model. MBio. 2019;10(2).
27. Vargas G, Rocha JD, Oliveira DL, Albuquerque PC, Frases S, Santos SS, et al. Compositional and immunobiological analyses of extracellular vesicles released by Candida albicans. Cellular microbiology. 2015;17(3):389–407. [PubMed: 25287304]
28. Bitencourt TA, Rezende CP, Quaresemin NR, Moreno P, Hatanaka O, Rossi A, et al. Extracellular Vesicles From the Dermatophyte *Trichophyton interdigitale* Modulate Macrophage and Keratinocyte Functions. Frontiers in immunology. 2018;9:2343. [PubMed: 30356863]
29. Peres da Silva R, Heiss C, Black I, Azadi P, Gerlach JQ, Travassos LR, et al. Extracellular vesicles from Paracoccidioides pathogenic species transport polysaccharide and expose ligands for DC-SIGN receptors. Scientific reports. 2015;5:14213. [PubMed: 26387503]

30. Liu S, Hossinger A, Hofmann JP, Denner P, Vorberg IM. Horizontal Transmission of Cytosolic Sup35 Prions by Extracellular Vesicles. MBio. 2016;7(4).

31. Zarnowski R, Sanchez H, Covelli AS, Dominguez E, Jaromin A, Bernhardt J, et al. *Candida albicans* biofilm-induced vesicles confer drug resistance through matrix biogenesis. PLoS biology. 2018;16(10):e2006872. [PubMed: 30296253]

32. Guimaraes AJ, Frases S, Gomez FJ, Zancope-Oliveira RM, Nosanchuk JD. Monoclonal antibodies to heat shock protein 60 alter the pathogenesis of Histoplasma capsulatum. Infection and immunity. 2009;77(4):1357–67. [PubMed: 19179416]

33. Rosenow EC. Focal infection with special reference to oral sepsis. Journal of Dental Research. 1919:205–49.

34. Shen Q, Beucler MJ, Ray SC, Rappleye CA. Macrophage activation by IFN-gamma triggers restriction of phagosomal copper from intracellular pathogens. PLoS pathogens. 2018;14(11):e1007444. [PubMed: 30452484]

35. Christie WW. Sphingomyelin and Related Sphingophospholipids Dundee, Scotland: LIPID MAPS; 2019 [Available from: https://www.lipidmaps.org/resources/lipidweb/index.php?page=lipids/sphingo/sph/index.htm.

36. Estruch F Stress-controlled transcription factors, stress-induced genes and stress tolerance in budding yeast. FEMS Microbiology Reviews. 2000;24(4):469–86. [PubMed: 10978547]

37. François J, Parrou JL. Reserve carbohydrates metabolism in the yeast *Saccharomyces cerevisiae*. FEMS Microbiology Reviews. 2001;25(1):125–45. [PubMed: 11152943]

38. Hare PD, Cress WA, Van Staden J. Dissecting the roles of osmolyte accumulation during stress. Plant, Cell & Environment. 1998;21(6):535–53.

39. Thammahong A, Puttikamonkul S, Perfect JR, Brennan RG, Cramer RA. Central Role of the Trehalose Biosynthesis Pathway in the Pathogenesis of Human Fungal Infections: Opportunities and Challenges for Therapeutic Development. Microbiology and Molecular Biology Reviews. 2017;81(2):e00053–16. [PubMed: 28298477]

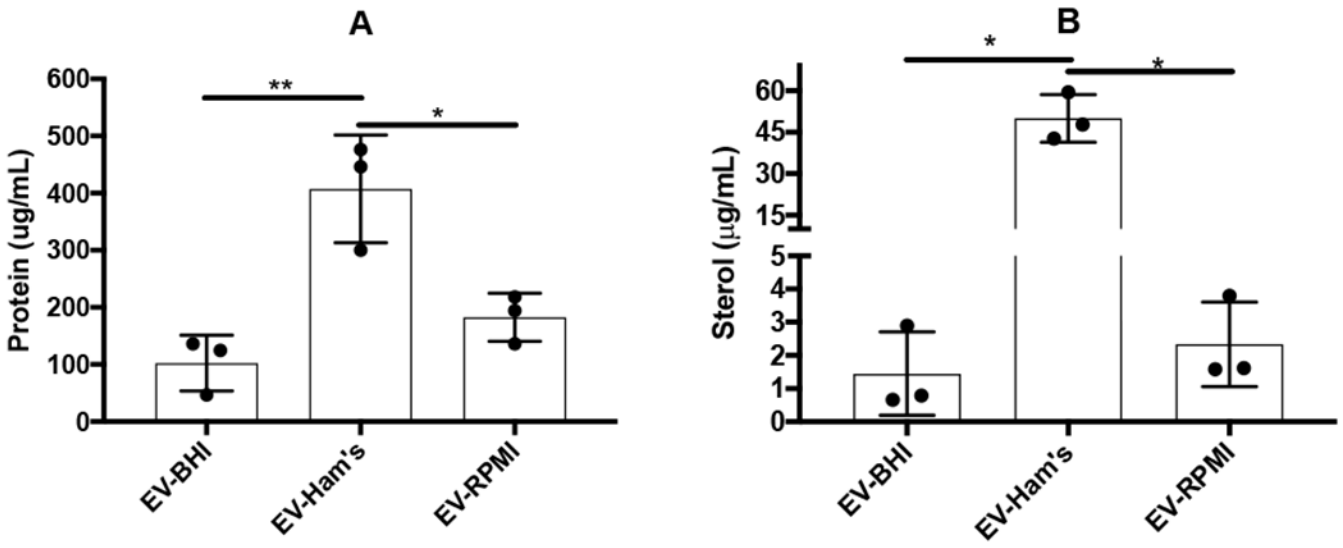

Figure 1. Protein and ergosterol content of EVs from *H. capsulatum* grown in distinct media.
The graph shows the protein (A) and ergosterol (B) quantifications of EV isolated from each culture supernatant. Graphs represent average and standard deviations for at least 3 independent EV isolations. * = $p < 0.05$, ** = $p < 0.01$, by Tukey multiple comparison test.

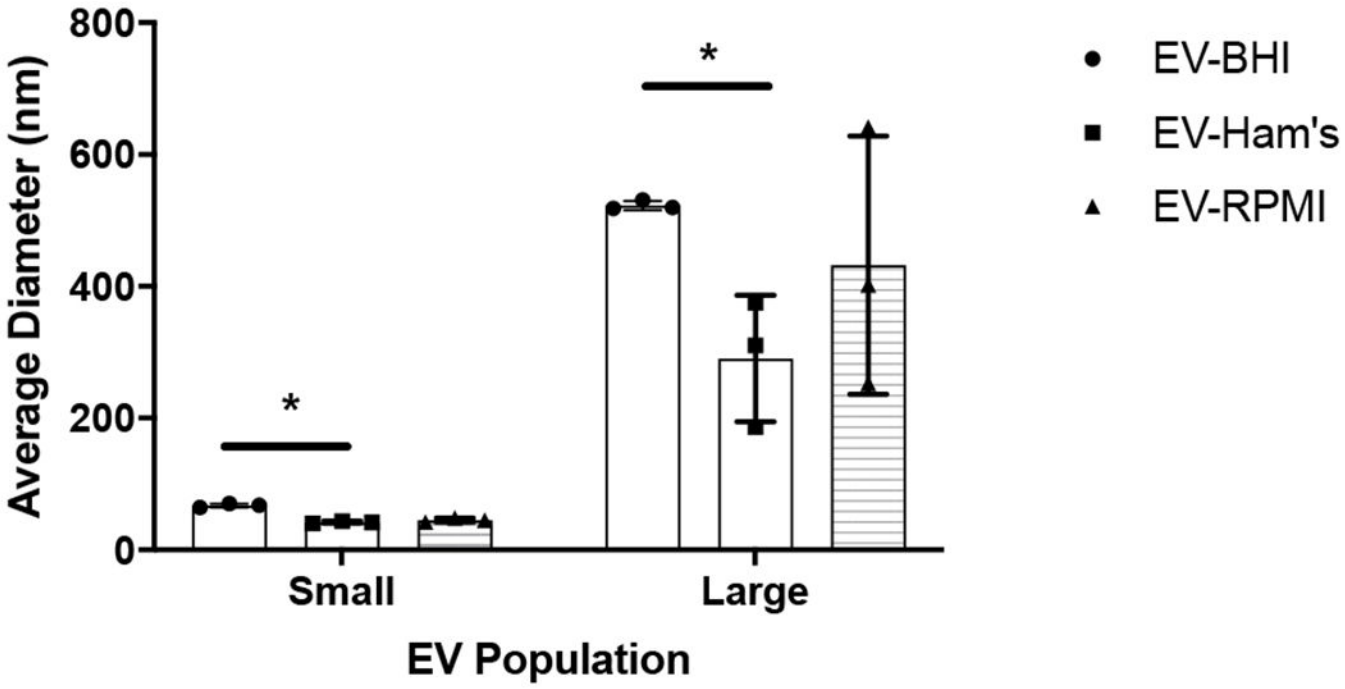

Figure 2. Size of EVs cultivated in distinct media by DLS.

After their isolation from medium supernatant, EVs were analyzed by Dynamic Light Scattering. The graph shows average and standard deviation for samples from 3 independent experiments. * = $p < 0.05$ by ANOVA followed by Tukey's multiple comparison test.

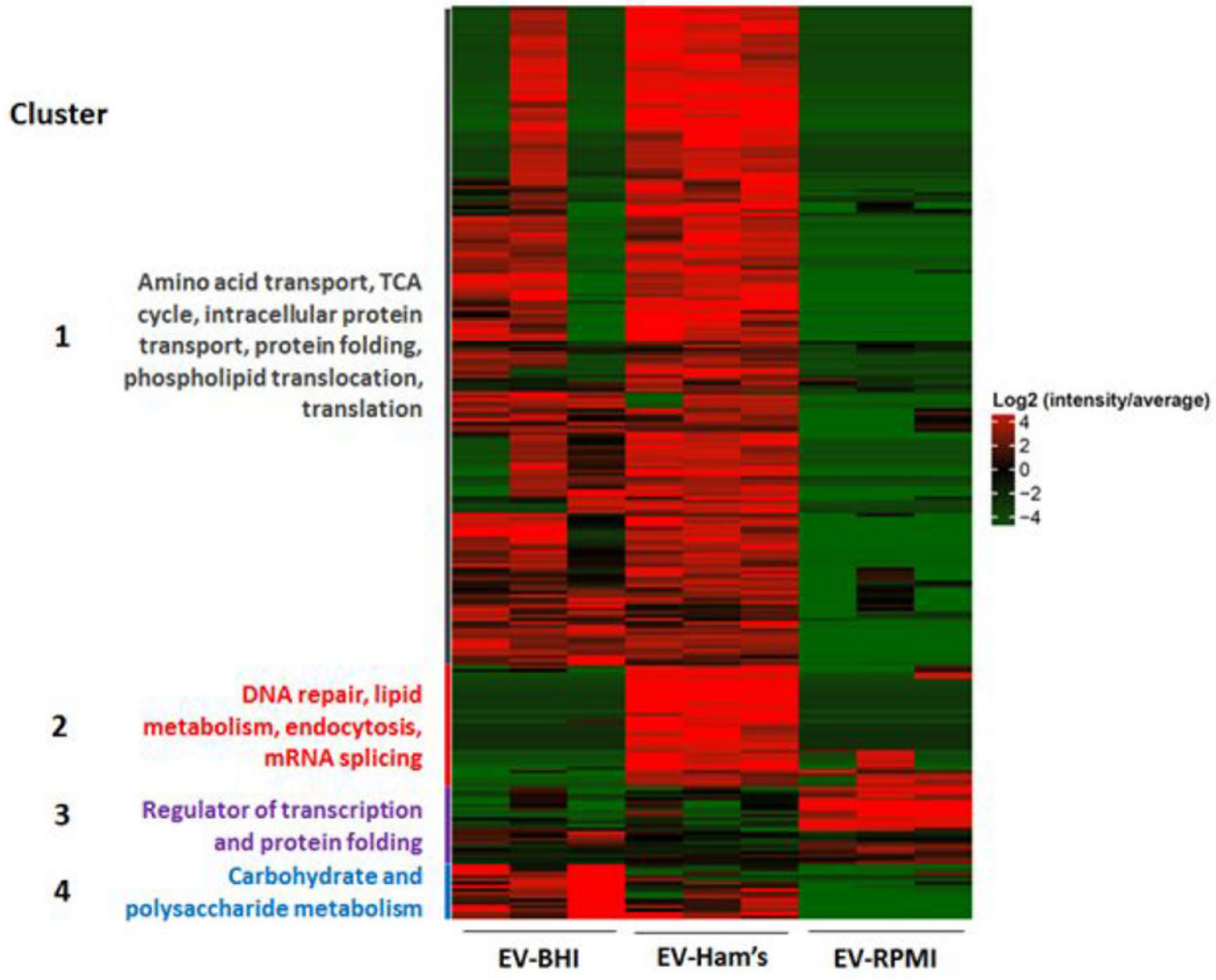

Figure 3. EV proteins in different media conditions.

The heatmap shows differential abundance of proteins in EVs produced by *H. capsulatum* yeast cells cultivated in distinct media. Proteins were grouped based on function. Group 1: Amino acid transport, TCA cycle, intracellular protein transport, phospholipid translocation, and translation. Group 2: DNA repair, lipid metabolism, endocytosis, and mRNA splicing. Group 3: Transcription regulators and protein folding. Group 4: Carbohydrate and polysaccharide metabolism

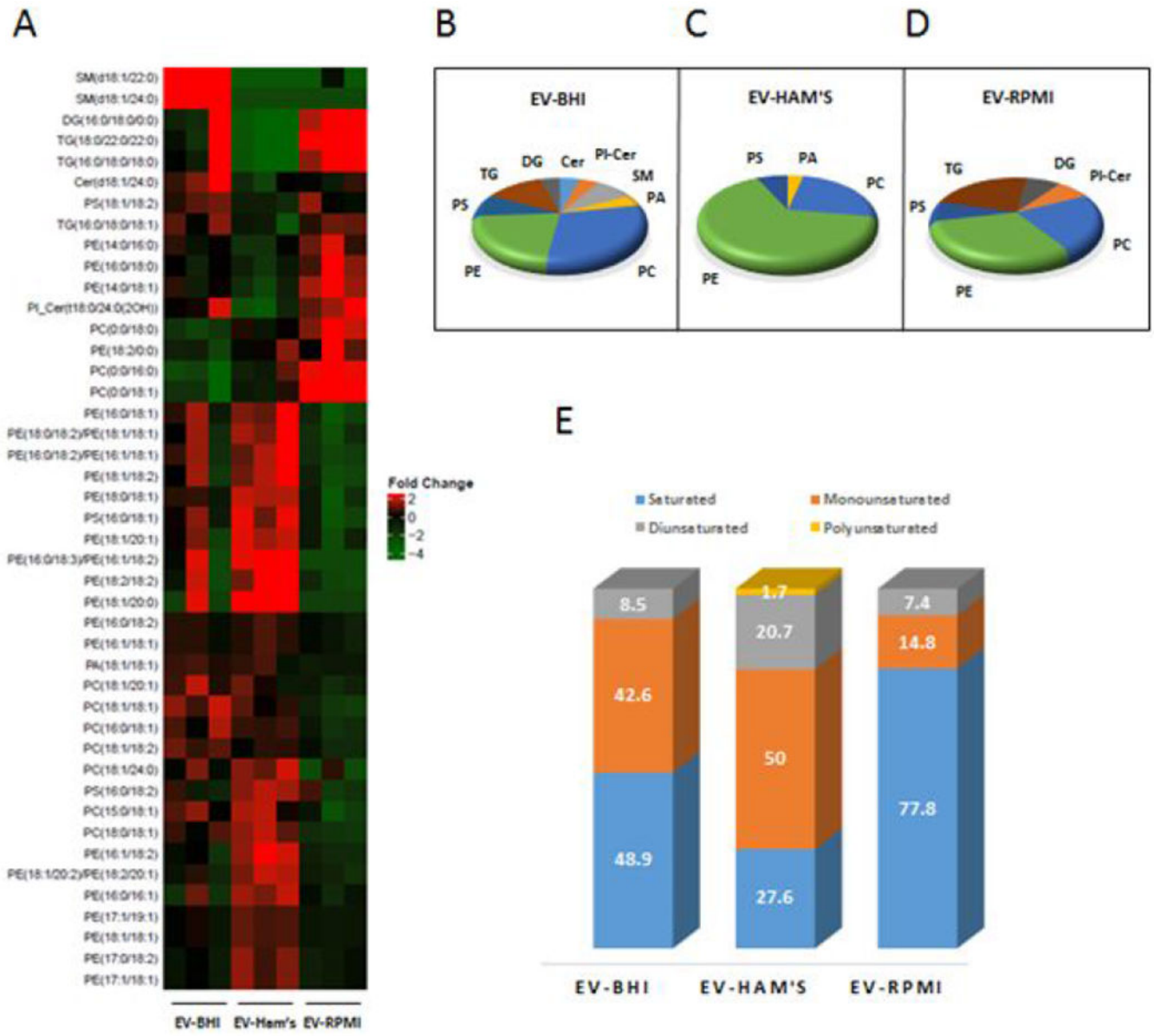

Figure 4.

Heatmap with lipids significantly altered in EVs released by *H. capsulatum* cultured under different media.

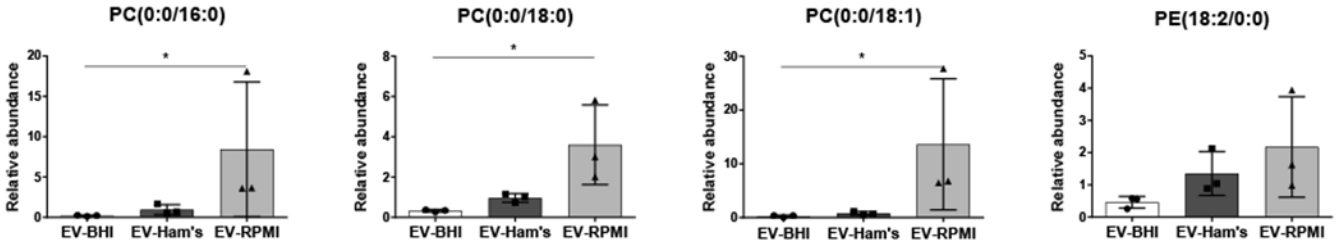

Figure 5. Lysophospholipids in EVs from *H. capsulatum* grown in different media.

This figure shows the abundance of distinct lysophospholipids found in each condition. Significant differences were found between EV-RPMI and EV-BHI. * = $p < 0.05$ by one-way ANOVA followed by Dunn's multiple comparisons test.

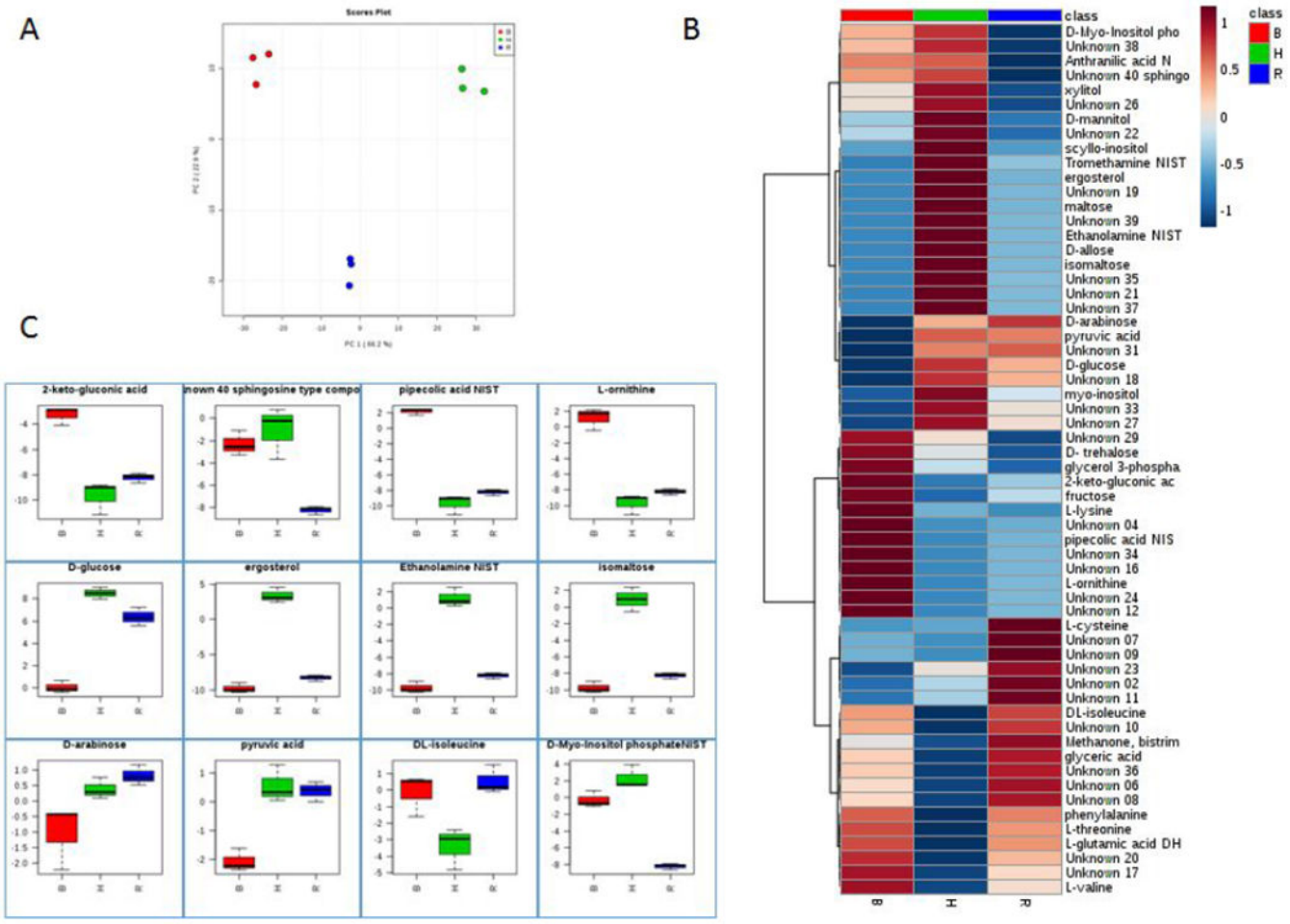

Figure 6. Metabolic pathways affected by different media.

The PCA plot (A) illustrates the distinction between the metabolic profiles of EVs from different media. In the heatmap (B) the metabolites detected in EVs from *H. capsulatum* cultivated in different media. Some of the detected metabolites were depicted (C) to show their variation among EVs from different growth conditions.

Table 1.

KEGG pathways affected by distinct culture conditions

Map Description	Fold Enrichment	Fisher test
Other types of O-glycan biosynthesis	25.59	9.7E-05
Fatty acid biosynthesis	10.24	2.4E-03
Fatty acid degradation	10.04	9.1E-05
Pyruvate metabolism	9.75	8.6E-07
Arginine biosynthesis	9.48	1.2E-04
Citrate cycle (TCA cycle)	7.58	9.6E-05
Alanine, aspartate and glutamate metabolism	7.06	1.5E-04
Oxidative phosphorylation	6.52	5.3E-10
Amino sugar and nucleotide sugar metabolism	6.46	7.4E-05
Fatty acid metabolism	6.32	8.8E-04
2-Oxocarboxylic acid metabolism	5.17	2.2E-03
Propanoate metabolism	5.12	1.7E-02
Glyoxylate and dicarboxylate metabolism	5.06	6.4E-03
Ribosome	4.88	7.4E-07
Peroxisome	4.88	4.4E-04
Starch and sucrose metabolism	4.88	7.3E-03
Valine, leucine and isoleucine degradation	4.71	8.2E-03
Glycolysis / Gluconeogenesis	4.27	1.1E-02
Phenylalanine metabolism	4.27	2.7E-02
Carbon metabolism	4.22	2.0E-05
Aminoacyl-tRNA biosynthesis	4.16	5.4E-03
Endocytosis	4.14	5.3E-04
Protein processing in endoplasmic reticulum	4.10	2.6E-04
Biosynthesis of antibiotics	3.94	6.5E-09
Biosynthesis of amino acids	3.86	4.7E-05
Biosynthesis of secondary metabolites	3.73	1.5E-10
Metabolic pathways	3.49	3.9E-23